



HAL
open science

Force-Driven Polymerization and Turgor-Induced Wall Expansion

Olivier Ali, Jan Traas

► **To cite this version:**

Olivier Ali, Jan Traas. Force-Driven Polymerization and Turgor-Induced Wall Expansion. Trends in Plant Science, 2016, 21 (5), pp.398 - 409. 10.1016/j.tplants.2016.01.019 . hal-01396586

HAL Id: hal-01396586

<https://hal.science/hal-01396586>

Submitted on 12 Oct 2018

HAL is a multi-disciplinary open access archive for the deposit and dissemination of scientific research documents, whether they are published or not. The documents may come from teaching and research institutions in France or abroad, or from public or private research centers.

L'archive ouverte pluridisciplinaire **HAL**, est destinée au dépôt et à la diffusion de documents scientifiques de niveau recherche, publiés ou non, émanant des établissements d'enseignement et de recherche français ou étrangers, des laboratoires publics ou privés.

1 **Force-driven polymerization and turgor-induced wall**
2 **expansion**

3 Olivier Ali^{1,2}, Jan Traas¹

4 *Present address and affiliation:*

5 1. Laboratoire de Reproduction et Développement des Plantes, Université Claude Bernard Lyon
6 1, ENS- Lyon, INRA, CNRS, Lyon, France

7 2. Virtual Plants Inria team, UMR AGAP, CIRAD, INRIA, INRA, Montpellier,

8 *Corresponding Authors:* Traas, J. (jan.traas@ens-lyon.fr), Ali, O. (olivier.ali@ens-lyon.fr)

9 **Abstract**

10 While many molecular players involved in growth control have been identified in the past
11 decades, it is often unknown how they mechanistically act to induce specific shape changes
12 during development. Plant morphogenesis results from the turgor-induced yielding of the
13 extracellular, load-bearing cell wall. Its mechano-chemical equilibrium appears as a fundamental
14 link between molecular growth regulation and the effective shape evolution of the tissue. Here,
15 we focus on force-driven polymerization of the cell wall as a central process in growth control.
16 We propose that mechanical forces facilitate the insertion of wall components, in particular
17 pectins, a process that can be modulated through genetic regulation. We formalize this idea in a
18 mathematical model, which we subsequently challenge with published experimental results.

19 **Introduction**

20 The link between gene regulation and growth, *i.e.* the irreversible spatial expansion of a cell or a
21 tissue, is a major issue in plant and animal developmental biology. However, although many
22 genetic regulators of morphogenesis have been identified, it is not clear how their activities
23 precisely translate into chemical and physical changes within the cells and consequently into
24 tissular morphogenesis. Here we will focus on the transduction between chemical and mechanical
25 energies, which is at the heart of this multi-scale process.

26 The particularities of plant growth and morphogenesis find their origin within the structure of
27 plant cells themselves, which can be considered as pressurized fluid droplets surrounded by a
28 stiff cell wall. In order to grow, cells must expand their wall in an irreversible manner. Early
29 work by *e.g.* Ray *et al* [1] provided evidence that wall expansion depends on chemical and
30 metabolic regulation, as opposed to a situation where turgor would simply induce growth by
31 breaking bonds between molecules. The current view is, that molecular networks that regulate
32 morphogenesis in plants have to interfere with the chemical structure of their wall, making it
33 yield to the internal turgor pressure at particular rates and in particular directions. To this end, the
34 role of transcriptional and post-transcriptional regulators in growth control can be understood in
35 terms of local wall remodeling.

36 From a thermodynamics perspective, plant morphogenesis can be seen as the result of an
37 interplay between turgor-generated mechanical energy and the chemical reactions leading to cell
38 wall expansion. Several conceptual frameworks have been developed to describe and analyze this
39 complex process ([2] for review, see also: [3], [4]). In this context, Barbacci *et al* exposed a
40 general thermodynamics framework to describe the coupling between mechanical and chemical

41 energies [5]. In the present opinion paper we take this approach further by showing how a
42 specific biochemical and biomechanical process, force-driven polymerization, fits into this
43 framework.

44 Up to now, the coupling between mechanics and growth is usually considered from a large scale
45 perspective, individual walls being described as a continuous material, characterized by
46 rheological properties (see Glossary) such as elasticity or viscosity [6-8]. Hereby, growth
47 mechanisms are usually grasped through phenomenological equations similar to the ones
48 depicting plasticity in non-living materials. These continuum mechanics-based approaches are
49 very powerful as they benefit from existing simulation tools and concepts for the study of non-
50 biological materials. Despite the usefulness of such models, however, their large-scale focus is
51 also their limitation, for no attention is really paid to the underlying molecular mechanisms. As a
52 result, molecular regulations are abstractly interpreted as modulations of rheological variables.
53 Therefore it remains difficult to link experimentally measured transcriptional control or
54 enzymatic activity to observed growth patterns. Moreover, useful and intuitive interpretations of
55 underlying molecular functions such as repair mechanisms, self-assemblies, *etc.*, are out of reach.
56 We therefore need, in addition, more mechanistic models for growth, including the detailed
57 molecular structure of the wall, explicitly linking molecular components to the overall
58 rheological properties.

59 We therefore investigated if, from a simplified description of the molecular content of the wall,
60 we could integrate a large-scale consecutive law of growing plant cells, which could then be used
61 to characterize the function of individual molecular regulators.

62 We argue here, that mechanical forces generated by turgor could facilitate the insertion of wall

63 components. Such a coupling between mechanics and biochemistry, termed force-driven
64 polymerization, has also been described for the assembly of actin bundles in animal systems [9].
65 Starting from known descriptions of cell wall structure (see [10] and references therein) we
66 expose how force-driven polymerization could be central in scaling up molecular processes into
67 viscoplastic behavior and ultimately growth of multicellular structures.

68 **The cell wall is a fiber-reinforced hydrogel**

69 The cell wall is composed of a network of rigid cellulose microfibrils embedded in a matrix,
70 mostly composed of water, polysaccharides such as pectins and hemicelluloses, proteins and ions
71 [11]. This matrix corresponds to a biphasic mixture between a porous solid phase and a liquid
72 one [12]. Therefore, the cell wall as a whole can be considered as a fiber-reinforced hydrogel.

73 From a functional point of view, the wall performs two contrasting functions, as it has to resist
74 turgor-induced constraints whereas simultaneously it should be able to expand. Because of their
75 mechanical characteristics [13,14], the cellulose microfibrils tethered to each other by shorter
76 hemicellulose chains are major actors in both of these functions (for reviews see: [10,15] [16].
77 The available experimental evidence suggests that cellulose microfibrils deposition is involved in
78 growth inhibition rather than in growth promotion *per se*. Indeed, after drug-induced inhibition of
79 cellulose deposition, cells can continue to grow during several tens of hours [17,18]. Similarly,
80 growth also occurs in certain mutant backgrounds where cellulose synthesis is impaired [19,20].
81 These experimental clues suggest that growth of the cell wall relies on the expansion of the
82 embedding matrix. In other words a scenario has emerged, where cell wall expansion is restricted
83 by the synthesis of cellulose microfibrils and promoted by the synthesis of matrix material. In the
84 following paragraphs we will discuss an important component of this matrix, *i.e.* pectin. As we

85 will see, there is increasing evidence that pectin could play an important role in growth control.

86 **Pectin is an important structural component of the wall matrix**

87 As indicated above, hemicelluloses such as xyloglucans have been classically considered as
88 essential structural components, central to concepts of wall loosening and induction of growth.
89 However, the recently produced *Arabidopsis thaliana* double mutant (*xxt1/xxt2*), showing a loss
90 of xyloglucan synthesis, does not show major growth deficiencies [21,22], suggesting that the
91 irreversible expansion of the cell wall does not rely, at least totally, on hemicellulose dynamics
92 only. This has revived the interest in the role of pectins in growth control. Pectins form up to 35
93 % of the primary cell wall of dicots [11] - *i.e.* the wall surrounding young and fast growing cells.
94 Their dynamics have been associated with growth control in several cell types, in particular tip-
95 growing cells such as pollen tubes and root hairs, for review see [10] and references therein, see
96 also *e.g.* [23], [24]. Moreover, AFM-based assays on *Arabidopsis thaliana*, demonstrated that
97 pectin demethyl-esterification was required and tightly regulated during cell wall softening prior
98 to aerial organ outgrowth [25], [26]. In addition, recent evidence indicates the existence of close
99 interactions between cellulose and pectins which could function as tethers between the
100 microfibrils [15,27]. Dwarf phenotypes in mutants where pectin synthesis or delivery is impaired
101 further illustrate the importance of pectin production for plant growth [28,29]. Noteworthy,
102 pectins have also been identified as important regulators of growth in more primitive plants such
103 as the green algae [30,31].

104 Pectins are produced in the Golgi and exocytosed within the cell wall. They are composed of four
105 different polysaccharides: Homogalacturonan, Rhamnogalacturonan I, Rhamnogalacturonan II
106 and Xylogalacturonan. Different pectin molecules correspond to various combinations of those

107 three residues covalently attached together. Hereby, homogalacturonans stand out, for they
108 roughly account for 65% of all of them [32]. A fundamental feature of homogalacturonans is
109 their ability to form multiple intermolecular chelation bonds in presence of calcium cations.
110 These cations-dependent bonds are able to glue together pectin molecules, forming structures
111 called “egg-boxes” (Fig.1). In a cation-rich environment, these adhesive interactions lead to the
112 formation of a hydrogel [33]. In addition, pectins are able to interact with other cell wall
113 components including cellulose and hemicellulose [34].

114 An interesting feature is that newly synthesized homogalacturonans cannot spontaneously form
115 egg-box structures. Indeed, in order to trap divalent cations, the carboxyl groups of the
116 homogalacturonan chains must be negatively charged. When synthesized, carboxyl residues are
117 shielded by methyl groups, which must be removed to induce gelification. Therefore, two types
118 of pectin molecules can be distinguished: (i) “inactive” methyl-esterified M-pectin and (ii)
119 “active”, demethyl-esterified pectin, able to aggregate into macromolecular assemblies.
120 Demethyl-esterification is carried on within the cell wall by specialized enzymes, the pectin
121 methyl-esterases (PMEs). In turn, PME-inhibitors (PMEIs) can modulate PME activity. This
122 process is essential, for both the degree and the pattern of demethyl-esterification influence the
123 mechanical/rheological properties of the constituted gel [35]. Accordingly, modifications in the
124 levels of PME and PMEI expression significantly alter growth rates [36]. Note that other charged
125 residues such as acetyl-esters [11] can also be present on homogalacturonans and their regulation
126 could play a similar role. However, for the sake of simplicity we only consider methyl-ester
127 groups here. Noteworthy, 66 PMEs and 69 PMEIs have been reported in the Arabidopsis
128 genome, attesting for the importance of the process [33,37]. The PME/PMEI system appears as a
129 key regulator of cell wall expansion:

- 130 • First, by regulating the amount of “active” demethyl-esterified pectins, within the matrix
131 liquid phase, ready for insertion it influences its viscosity: The more active molecules
132 available, the faster the expansion.
- 133 • Secondly, by removing more or less methyl groups on pectin molecules already stuck
134 together, it regulates the strength of the bonds within the matrix solid phase. This can be
135 interpreted as the tuning of the plastic yielding threshold of the cell wall.

136 In conclusion, in the previous paragraphs we have seen that the cell wall can be considered as a
137 fiber reinforced hydrogel, which is put under tension by the osmotic pressure within the cells. To
138 grow, the cells have to yield to this pressure by expanding their walls in an irreversible manner.
139 We will next discuss the chemical and physical processes that are at the basis of this expansion,
140 before indicating how molecular regulation can act to generate specific shapes of tissues and
141 organs. To be able to go beyond qualitative descriptions of growth regulation, we will present a
142 description in the form of a mathematical model. Finally we test this model using available
143 quantitative data

144 **Chemical equilibrium of the pectin hydrogel**

145 If single molecules in solution can bind to each other, macromolecular assemblies are generated.
146 Assuming a high enough initial concentration of those molecules, such a mechanism eventually
147 leads to the formation of a hydrogel, *i.e.* the percolation of a macromolecular solid phase within a
148 solution of single molecules. The pectin matrix corresponds to such a biphasic system [12]. When
149 the cell is growing, new matrix material has to be added: new components are exocytosed within
150 the liquid phase and components from the liquid phase have to be transferred into the solid one.
151 Because the wall is a closed shell of constant thickness (*i.e.* with no border where an hypothetical

152 nucleation mechanism could take place), a way to add new components to the solid phase is by
153 inserting them in between existing ones. Such a mechanism is sketched in Fig.1a and formalized
154 in Eq.1, where N_b and M respectively depict one bond between two molecules in the solid phase
155 and a free molecule in the liquid one.



157 This chemical equilibrium between the liquid and solid phase of the gel can be formalized by
158 standard concepts from thermodynamics. Indeed, phase equilibrium is reached once the *free*
159 energy (we will drop the “*free*” for now on) difference $\Delta E (= E_{bound} - E_{unbound})$ between the
160 two sides of Eq.1 vanishes. This energy difference reads $\Delta E = E_b - k_B T \cdot \ln(c/c_0)$ and
161 encompasses two general classic features. First, the stabilization of molecules by the adhesive
162 interactions between them is accounted for by the first term $E_b < 0$ (the negative sign meaning
163 that adhesion stabilizes the system, *i.e.* lowers its energy). Second, the insertion of one molecule
164 from the liquid phase into the solid one comes with the loss of some degree of freedom. This is
165 expressed by the second term $-k_B T \cdot \ln(c/c_0)$ a standard expression of mixing entropy, where
166 $k_B T$ represents the thermal energy of the system (k_B and T respectively stand for the Boltzmann
167 constant and the absolute temperature), c depicts the monomer concentration in the liquid phase
168 and c_0 the water concentration in that same phase ($\simeq 55 \text{ mol} \cdot \text{L}^{-1}$). In view of the above, the
169 equilibrium condition $\Delta E = 0$ provides a value for a corresponding critical free molecule
170 concentration (with $\beta = 1/k_B T$):

171
$$c_0^* = c_0 \cdot \exp(\beta E_b) \quad (2)$$

172 In other terms, the actual concentration c of monomers in solution controls the chemistry of the

173 gel:

174 • If $c > c_0^* \Leftrightarrow \Delta E < 0$, monomers spontaneously insert into the solid phase, growth
175 occurs.

176 • If $c < c_0^* \Leftrightarrow \Delta E > 0$, no spontaneous insertion, no growth occurs.

177 The critical concentration c_0^* only depends on one parameter: the adhesive energy between
178 molecules in the solid phase (E_b in Eq.2). In order to modulate this equilibrium the cell only has
179 to tune the adhesive links between molecules. This can be achieved using enzymatic activities,
180 *i.e.* through molecular regulation. However, another efficient way to do so is by pulling on those
181 links (Fig.1), as detailed in the following paragraph.

182 **Influence of mechanical forces on the chemical equilibrium**

183 A tensile force (f) applied on the solid phase can ease the breaking of existing bonds, thus
184 facilitating the insertion of soluble molecules. This shifts the chemical equilibrium towards
185 polymerization — *i.e.* towards the right-hand side of Eq.1. In this case, the energy difference has
186 to be lowered by the work $w = f \cdot a$ generated by the tensile force (f) over a distance a ,
187 characteristic of the deformation of loaded bonds: $\Delta E' = \Delta E - f \cdot a$. Consequently, the
188 equilibrium condition $\Delta E' = 0$ yields, this time, a force-dependent expression for the equilibrium
189 concentration c^* :

190
$$c^*(f) = c_0^* \cdot e^{-\beta \cdot f \cdot a} \quad (3)$$

191 This mechanism assures that tensile forces applied on a gel at equilibrium decrease its critical
192 concentration. As a consequence molecules in solution are recruited into the solid phase, (Fig.1 &

193 2). This transduction mechanism is called force-induced polymerization and has been shown to
194 play an important role in the dynamics of major load-bearing structures such as the actin
195 cytoskeleton [38-41]. Note that this mechanism is by essence irreversible, for when an increased
196 force is applied on a given configuration (black arrow on Fig.2a) and then removed (dashed black
197 arrow on Fig.2a) the system does not go back to its original position.

198 **Linking mechanics and biochemistry to geometry: spatial expansion** 199 **of the pectin matrix under tensile force**

200 One difference between the growth of living tissues and the plasticity of non-living materials is
201 the mass increase of the former. Therefore, it seemed logical to seek for a growth law based on
202 the equation of mass conservation of the solid phase of the matrix (see Box 1 for details).
203 Formalizing the fact that the local expansion of the matrix is fuelled by the insertion mechanism
204 previously exposed yields (combination of Eq. 2, 3 & B1-4):

$$205 \quad R_g = K \cdot \delta c \cdot e^{\beta(f \cdot a - E_b)} \quad (4)$$

206 where the relative expansion rate (R_g) is expressed as a function of the tensile force (f),
207 formalizing the out-of-equilibrium insertion reaction. $K > 0$ is a proportionality constant and δc
208 represents the excess of free monomer in solution compared to the equilibrium concentration.
209 Note that in an exhaustive approach the coefficient K should depend on the elastic energy stored
210 in the solid phase. But in a turgid growing tissue this stored energy should be roughly constant
211 and can be ignored for the sake of simplicity.

212 **Reinforcing the gel: the cellulose microfibrils network steps in**

213 Eq.4 depicts the expansion of a hydrogel under mechanical load, applied to the specific case of
214 pectin within the cell wall. A corollary question concerns the integration of the cellulose
215 microfibril network in this description.

216 The entanglement between the pectin-based matrix and the cellulose fibrils leads to a complex
217 distribution of mechanical constraints at the molecular scale. An accurate mechanical analysis
218 would require a precise structural description of the considered wall and intensive numerical
219 simulations, similar to the ones produced by Kha *et al* [42] and Puri *et al* [43] in the case of cell
220 wall models containing only cellulose and hemi-cellulose fibers. Such a study lies outside of the
221 range of this article and we will only provide a qualitative analysis here.

222 In a wall containing both pectin and cellulose, the force (f) felt by a pectin strand in a given
223 direction should in principle only be a fraction of the total force (f_{tot}) exerted on a unit volume of
224 the wall. This fraction would depend, at the very least, on the relative concentration of cellulose
225 fibers compared to pectin strands (r_{c-p}) and the rigidity of those fibers (Y_c):

$$226 \quad f = f(f_{tot}, r_{c-p}, Y_c) \leq f_{tot} \quad .$$

227 Controlling both the angular distribution of cellulose fibers and their rigidity appears as a way to
228 regulate the force exerted on pectin strands and consequently the expansion rate (R_g) as
229 expressed in Eq.4. Following this idea, two stereotypical asymptotic cases can be evoked:

- 230 • All the cellulose fibers are oriented perpendicular to the expanding pectin strand (*c.f.* Fig.
231 1b-2). In this case, the cellulose fibers and the pectin strand can be considered in series
232 and the whole force exerted on the wall is transmitted to the strand: $f = f_{tot}$.
- 233 • All the cellulose fibers are oriented in the same direction as the expanding pectin strand

234 (c.f. Fig 1b-3). In this case, the cellulose fibers and the pectin strand lie in parallel and the
235 force felt by the pectin strand is smaller than the total one: $f \approx f_{tot}/(1 + r_{c-p} \cdot r_Y)$ where
236 r_{c-p} and r_Y respectively account for the ratio of relative concentrations of pectin and
237 cellulose and the rigidity ratio between a pectin strand and a cellulose fiber.

238 The qualitative point we want to make here is that enhancing the deposition of cellulose in a
239 given direction should directly down-regulate the expansion rate of the matrix in this specific
240 direction.

241 Finally, it is worth mentioning that a detailed thermodynamical description of such a fiber-
242 reinforced hydrogel should not only include dissipation between matrix molecules but also
243 between the fibers themselves and between the fibers and the matrix.

244 **Experiments on Chara fit the force-driven polymerization model**

245 We were not aware of quantitative experimental studies on higher plants focused on the
246 relationship between molecular composition of the cell wall, turgor-generated forces and the
247 morpho-dynamics of the whole tissue. Fortunately, such studies have been conducted on the
248 green algae *Chara corallina* [44,45] and we confronted the results with our model (Fig.3).

249 In the case of isolated Chara cells, the mechanical force (f) exerted on the cell wall is
250 proportional to the pressure differential (ΔP) between the inside and the outside of the wall.
251 Combined with Eq.4, this yields an exponential relationship between the pressure differential
252 exerted on a cell wall and its expansion rate. All other parameters kept constant, the ratio between
253 two relative growth rates (R_g/R_g^0) as a function of the corresponding ratio of pressure
254 differentials ($\Delta P/\Delta P_0$) reads:

255
$$\frac{R_g}{R_g^0} = \exp\left(C_1 \cdot \Delta P_0 \cdot \left(\frac{\Delta P}{\Delta P_0} - 1\right)\right) \quad (5)$$

256 see Fig.3a for a comparison between experimental points and the fitting function.

257 If we assume that the insertion of demethyl-esterified pectins is the molecular mechanism behind
258 cell wall expansion, the growing rate is an affine function of the concentration of demethyl-
259 esterified pectin molecules in the solute phase. Fig.3b depicts this behavior and qualitatively
260 matches experimental evidence of this proportionality exposed on Fig.3 of [45]: putting Chara
261 cells in a pectin-enriched solution increased their growing response to mechanical stress.

262 Another qualitative feature of Chara growth observed by Proseus *et al* and reproduced by our
263 model is its dependency on temperature: Fig 3c depicts how the pressure-growth rate relationship
264 is affected by a slight decrease of temperature (T), the shift from the plain curve to the dashed
265 one has to be compared to the shift between the two curves exposed on Fig.13 of [44]. These
266 qualitative agreements between our theoretical model and experimental data strengthen the idea
267 that force-driven assembly mechanisms of the cell wall matrix play an important role in cellular
268 growth.

269 **Discussion, perspectives & conclusion**

270 Our ambition was to demonstrate that a fundamental molecular mechanism (force-driven
271 polymerization) applied to a key actor (pectin) can be at the heart of a complex integrated
272 behavior such as morphogenesis.

273 Although force-driven insertion appears as an appealing mechanism to explain cell wall
274 expansion at the molecular scale, it is worth noting that it might not be the only one possible. For

275 instance, Rojas *et al* [23] proposed a detailed study of pollen tube expansion using an apposition
276 mechanism: Newly demethyl-esterified pectin molecules are not inserted into the solid phase but
277 rather directly polymerized as a new layer next to the old one. This new layer modifies the
278 mechanical properties of the load-bearing cell wall and induces its viscous relaxation. Such a
279 mechanism does not exclude the model we propose here but is rather complementary: Rojas *et al*
280 also describe a transduction mechanism between pectin chemistry and cell wall mechanics,
281 focusing their attention on the chemical control of the process. This shift of perspective between
282 their approach and ours (*i.e.* the question of causality between the chemical and the mechanical
283 states of the cell wall) is a molecular version of the debate between Linthillac and Schöpfer that
284 took place a few years back [46,47]: Is growth controlled by wall-loosening enzymes or by
285 turgor-induced stresses ? Our point is that what matters is the resulting equilibrium between both
286 ends which is formalized through the critical concentration Eq.3.

287 Force-driven polymerization processes have been proposed to play a major part in several
288 biological functions relying on active gel dynamics and mechano-chemical transduction, from
289 actin filament formation and focal adhesion formation [9], [41], [48] (Kozlov *et al*) in animal
290 cells to cell wall instability and cell division in bacteria [49]. In our opinion, force-driven
291 polymerization processes could be as central in mechanobiology as Michaelis-Menten
292 mechanisms in biochemistry.

293 Indeed, force-driven polymerization can be seen as a transduction mechanism between a
294 mechanical force and a chemical reaction. From a theoretical perspective, in its full 3D version
295 this mechanism provides a gateway to develop models that integrate quantitative geometrical
296 variables and biochemical equations (Fig.4). In other words, it becomes possible to express
297 molecular activities in terms of geometrical outputs at the level of entire tissues and organs in a

298 fully mechanistic manner. For this purpose, Eq.4 can be coupled to other differential equations
299 describing the dynamics of enzymatically-regulated variables. For instance one could assume that
300 the activation energy E_b in Eq.4 depends on the demethyl-esterification degree of pectin
301 molecules and that pectin methyl esterases regulate its value. The influence of PME activity on
302 growth by coupling Eq.4 could then be explored using an equation describing PME dynamics.

303 To assess the validity of the model a wide range of experiments can be considered. The first step
304 would be to extend the quantitative analysis produced by Proseus and Boyer to cells and tissues
305 from higher plants: quantitative tracking to follow cells and tissues submitted to various levels of
306 turgor pressure could be a start. In complement, rescue assays could be tested to restore a normal
307 growth phenotype to mutant or drug-treated plants by modulation of mechanical forces. Finally
308 and more speculatively, the use and analysis of biomimetic systems such as artificial walls could
309 also be very useful.

Bibliography

- 311 1 Ray, P.M. and Ruesink, A.W. (1962) Kinetic experiments on the nature of the growth
312 mechanism in oat coleoptile cells. *Dev. Biol.* 4, 377–397
- 313 2 Ali, O. *et al.* (2014) Physical models of plant development. *Annu. Rev. Cell Dev. Biol.* 30,
314 59–78
- 315 3 Kennaway, R. *et al.* (2011) Generation of Diverse Biological Forms through Combinatorial
316 Interactions between Tissue Polarity and Growth. *PLoS Comput Biol* 7, e1002071–22
- 317 4 Hamant, O. *et al.* (2008) Developmental Patterning by Mechanical Signals in Arabidopsis.
318 *Science* 322, 1650–1655
- 319 5 Barbacci, A. *et al.* (2013) Another Brick in the Cell Wall: Biosynthesis Dependent Growth
320 Model. *PLoS ONE*
- 321 6 Boudon, F. *et al.* (2015) A computational framework for 3D mechanical modeling of plant
322 morphogenesis with cellular resolution. *PLoS Comput Biol* 11, e1003950
- 323 7 Dyson, R.J. and Jensen, O.E. (2010) A fibre-reinforced fluid model of anisotropic plant cell
324 growth. *J. Fluid Mech.* 655, 472–503
- 325 8 Dumais, J. *et al.* (2006) An anisotropic-viscoplastic model of plant cell morphogenesis by
326 tip growth. *Int. J. Dev. Biol.* 50, 209–222
- 327 9 Kruse, J.F.J. (2004) Aster, Vortices and Rotating Spirals in Active Gels of Polar
328 Filaments. *Phys. Rev. Lett.* 92, 1–4
- 329 10 Wolf, S. *et al.* (2012) Growth Control and Cell Wall Signaling in Plants. *Annu. Rev. Plant*
330 *Biol.* 63, 381–407
- 331 11 Caffall, K.H. and Mohnen, D. (2009) The structure, function, and biosynthesis of plant cell
332 wall pectic polysaccharides. *Carbohydrate Research* 344, 1879–1900
- 333 12 Iijima, M. *et al.* (2005) Swelling behaviour of calcium pectin hydrogels by
334 thermomechanical analysis in water. *Thermochimica Acta* 431, 68–72
- 335 13 Vincent, J. (1999) From cellulose to cell. *Journal of Experimental Biology* 202, 3263–3268
- 336 14 Zhang, T. *et al.* (2013) Visualization of the nanoscale pattern of recently-deposited cellulose
337 microfibrils and matrix materials in never-dried primary walls of the onion epidermis.
338 *Cellulose* 21(2), 853–862
- 339 15 Cosgrove, D.J. (2014) Re-constructing our models of cellulose and primary cell wall
340 assembly. *Current Opinion in Plant Biology* 22, 122–131
- 341 16 Cosgrove, D.J. (1993) How do plant cell walls extend? *Plant Physiology* 102, 1–6
- 342 17 Heisler, M.G. *et al.* (2010) Alignment between PIN1 Polarity and Microtubule Orientation
343 in the Shoot Apical Meristem Reveals a Tight Coupling between Morphogenesis and Auxin
344 Transport. *PLoS Biol.* 8, e1000516
- 345 18 Pelletier, S. *et al.* (2010) A role for pectin de-methylesterification in a developmentally
346 regulated growth acceleration in dark-grown Arabidopsis hypocotyls. *New Phytologist* 188,
347 726–739
- 348 19 Fagard, M. *et al.* (2000) PROCUSTE1 Encodes a Cellulose Synthase Required for Normal
349 Cell Elongation Specifically in Roots and Dark-Grown Hypocotyls of Arabidopsis. *The*
350 *Plant Cell* 12, 2409–2423
- 351 20 Hématy, K. *et al.* (2007) A receptor-like kinase mediates the response of Arabidopsis cells
352 to the inhibition of cellulose synthesis. *Current Biology* 17, 922–931
- 353 21 Park, Y.B. and Cosgrove, D.J. (2012) A revised architecture of primary cell walls based on

354 biomechanical changes induced by substrate-specific endoglucanases. *Plant Physiology* 158,
355 1933–1943

356 22 Cavalier, D.M. *et al.* (2008) Disrupting two *Arabidopsis thaliana* xylosyltransferase genes
357 results in plants deficient in xyloglucan, a major primary cell wall component. *The Plant*
358 *Cell Online* 20, 1519–1537

359 23 Rojas, E.R. *et al.* (2011) Chemically Mediated Mechanical Expansion of the Pollen Tube
360 Cell Wall. *Biophysical Journal* 101, 1844–1853

361 24 Parre, E. and Geitmann, A. (2005) Pectin and the role of the physical properties of the cell
362 wall in pollen tube growth of *Solanum chacoense*. *Planta* 220, 582–592

363 25 Braybrook, S.A. and Peaucelle, A. (2013) Mechano-Chemical Aspects of Organ Formation
364 in *Arabidopsis thaliana*: The Relationship between Auxin and Pectin. *PLoS ONE* 8, e57813

365 26 Peaucelle, A. *et al.* (2015) The Control of Growth Symmetry Breaking in the *Arabidopsis*
366 Hypocotyl. *Current Biology* 25, 1746–1752

367 27 Wang, T. *et al.* (2015) Cellulose-Pectin Spatial Contacts Are Inherent to Never-Dried
368 *Arabidopsis* Primary Cell Walls: Evidence from Solid-State Nuclear Magnetic Resonance.
369 *Plant Physiology* 168, 871–884

370 28 Bouton, S. *et al.* (2002) QUASIMODO1 encodes a putative membrane-bound
371 glycosyltransferase required for normal pectin synthesis and cell adhesion in *Arabidopsis*.
372 *The Plant Cell Online* 14, 2577–2590

373 29 Gendre, D. *et al.* (2013) Trans-Golgi network localized ECHIDNA/Ypt interacting protein
374 complex is required for the secretion of cell wall polysaccharides in *Arabidopsis*. *The Plant*
375 *Cell* 25, 2633–2646

376 30 Proseus, T.E. and Boyer, J.S. (2006) Calcium pectate chemistry controls growth rate of
377 *Chara corallina*. *J. Exp. Bot.* 57, 3989–4002

378 31 Proseus, T.E. and Boyer, J.S. (2014) Pectate chemistry links cell expansion to wall
379 deposition in *Chara corallina*. *psb* 7, 1490–1492

380 32 Mohnen, D. and Bar-Peled, M. (2008) Cell wall polysaccharide synthesis. ... *the Plant Cell*
381 *Wall for ...*

382 33 Wolf, S. *et al.* (2009) Homogalacturonan Methyl-Esterification and Plant Development.
383 *Mol. Plant* 2(5), pp.851-860

384 34 Popper, Z.A. and Fry, S.C. (2008) Xyloglucan-pectin linkages are formed intra-
385 protoplasmically, contribute to wall-assembly, and remain stable in the cell wall. *Planta*
386 227, 781–794

387 35 Peaucelle, A. *et al.* (2011) Pectin-Induced Changes in Cell Wall Mechanics Underlie Organ
388 Initiation in *Arabidopsis*. *Current Biology* 21, 1720–1726

389 36 Peaucelle, A. *et al.* (2008) *Arabidopsis* phyllotaxis is controlled by the methyl-esterification
390 status of cell-wall pectins. *Curr. Biol.* 18, 1943–1948

391 37 Sénéchal, F. *et al.* (2014) Homogalacturonan-modifying enzymes: structure, expression, and
392 roles in plants. *J. Exp. Bot.* 65, 5125–5160

393 38 Kozlov, M.M. and Bershadsky, A.D. (2004) Processive capping by formin suggests a force-
394 driven mechanism of actin polymerization. *The Journal of Cell Biology* 167, 1011–1017

395 39 Courtemanche, N. *et al.* (2013) Tension modulates actin filament polymerization mediated
396 by formin and profilin. *Proc Natl Acad Sci USA* 110, 9752–9757

397 40 Shemesh, T. and Kozlov, M.M. (2007) Actin Polymerization upon Processive Capping by
398 Formin: A Model for Slowing and Acceleration. *Biophysical Journal* 92, 1512–1521

399 41 Shemesh, T. (2005) Focal adhesions as mechanosensors: A physical mechanism.

400 *Proceedings of the National Academy of Sciences* 102, 12383–12388
401 42 Kha, H. *et al.* (2010) WallGen, Software to Construct Layered Cellulose-Hemicellulose
402 Networks and Predict Their Small Deformation Mechanics. *Plant Physiology* 152, 774–786
403 43 Yi, H. and Puri, V.M. (2012) Architecture-Based Multiscale Computational Modeling of
404 Plant Cell Wall Mechanics to Examine the Hydrogen-Bonding Hypothesis of the Cell Wall
405 Network Structure Model. *Plant Physiology* 160, 1281–1292
406 44 Proseus, T.E. *et al.* (2000) Turgor, temperature and the growth of plant cells: using *Chara*
407 *corallina* as a model system. *J. Exp. Bot.* 51, 1481–1494
408 45 Proseus, T.E. and Boyer, J.S. (2007) Tension required for pectate chemistry to control
409 growth in *Chara corallina*. *J. Exp. Bot.* 58, 4283–4292
410 46 Wei, C. and Lintilhac, P.M. (2003) Loss of stability—a new model for stress relaxation in
411 plant cell walls. *Journal of theoretical biology* 224, 305–312
412 47 SCHOPFER, P. (2008) Is the loss of stability theory a realistic concept for stress relaxation-
413 mediated cell wall expansion during plant growth? *Plant Physiology* 147(3), 935–936 author
414 reply 936–938
415 48 Nicolas, A. *et al.* (2004) Cell mechanosensitivity controls the anisotropy of focal adhesions.
416 *Proceedings of the National Academy of Sciences* 101, 12520–12525
417 49 Jiang, H. *et al.* (2011) Mechanical Control of Bacterial Cell Shape. *Biophysj* 101, 327–335
418
419

420 **Boxes**

421 **Trends box:**

- 422 • Cellulose microfibrils have historically drained most of the attention of biomechanical
423 studies of the cell wall. Recent results, however, suggest that the soft pectin matrix in
424 which they are embedded might also play a significant role in the physico-chemical
425 equilibrium of growing cells.
- 426 • At the molecular scale, biophysicists have shown how mechanical forces applied on
427 molecular assemblies can modulate their chemical state and therefore initiate specific
428 biological responses.
- 429 • At the tissular scale, numerical simulation tools borrowed from material sciences are
430 increasingly used in developmental biology. Morphogenesis in plant tissues is particularly
431 suited for this kind of approach.
- 432 • Bridging the gap between the molecular and the tissular scales is a major challenge in
433 developmental biology, for it would help relating explicitly shape changes and specific
434 molecular actors.

435 **Glossary box:**

436 **Rheology:** Study of the deformation of matter at a mesoscopic or macroscopic scale.

437 **Viscosity:** Rheological/mechanical property that relates the deformation rate of a material to its
438 mechanical load. For a given loading force, the more viscous a material is the slower it will
439 deform. Note that its inverse is called extensibility and is often used in growth modeling.

440 **Thermal energy:** The portion of the energy of a system due to the random relative microscopic
441 movements of its components. Absolute temperature of the system is, by definition, a direct
442 measure of this internal energy. For living systems which temperature is around 300 K the usual
443 value of their thermal energy is: $\mathcal{E}_{th} \propto k_B T = 1/\beta \approx 4 \cdot 10^{-21} \text{J}$, where $k_B = 1.38 \cdot 10^{-23} \text{J} \cdot$
444 K^{-1} and $T = 300 \text{K}$ respectively stand for the Boltzmann constant and the absolute temperature.

445 **Work of a force:** Considering an object in motion and submitted to a force, the work developed
446 by this force corresponds to the scalar product between the force vector and the displacement
447 vector.

448 **Box 1: From matter conservation to force-induced expansion**

449 The conservation equation of the number of bonds in the solid phase reads:

450
$$\frac{dn_b}{dt} = -n_b R_g + s_b \quad (\text{B1-1})$$

451 The term of the left hand-side of Eq.B1-1 depicts the local time evolution of the bond
452 density (noted n_b). The first term of the right hand-side is proportional to the relative
453 expansion rate of the cell wall (R_g) and accounts for the fact that the matrix can expand.
454 The minus sign in front of it insures that spatial expansion of the matrix ($R_g > 0$) tends to
455 diminish the local bond density. Finally, the second term of the right hand-side (named
456 the source term and denoted s_b) grasps the chemical insertion mechanism that transfers
457 molecules from the liquid phase into the solid one when the two phases are out of
458 equilibrium.

459 Because the cell wall is constantly under tension, the spacing between molecules in the
460 solid phase and therefore the bond density can be assumed constant over time (*i.e.*
461 $dn_b/dt = 0$ in Eq.B1-1). This assumption implies that the two terms of the right hand-
462 side of Eq.B1-1 compensate each other, leading to a direct relationship between the
463 expansion rate of the cell wall and the pectin chemical insertion rate:

464
$$n_b R_g = s_b \quad (\text{B1-2})$$

465 The proper derivation of chemical insertion rate (s_b) from thermodynamical

466 considerations lies outside the range of this opinion article but in a few words it can be
467 estimated as follows. It should be proportional to the density of insertion sites (n_b) and to
468 the excess of free molecules in solution compared to equilibrium: $\delta c = c - c^*$. It
469 therefore corresponds to a relaxation term when the pectin molecules in the two phases
470 are out of equilibrium. If the system is only slightly out of equilibrium, this relaxation
471 flux can be linearized with respect to the chemical potential difference between the two
472 pectin phases ($\partial\Delta\mathcal{E}/\partial c|_{c^*}$ in Eq.B1-3) leading to the following expression:

473
$$s_b \propto - \left. \frac{\partial\Delta\mathcal{E}}{\partial c} \right|_{c^*} \cdot \delta c \cdot n_b \quad (\text{B1-3})$$

474 This yields the simple relationship between the relative spatial expansion rate of the wall
475 and the equilibrium concentration $c^*(f)$ that explicitly depends on the mechanical force f
476 as Eq.3 depicts:

477
$$R_g \propto \frac{1}{c^*(f)} \quad (\text{B1-4})$$

478 **Figures legends**

479 **Figure 1: Pectin strand dynamics & mechanical load distribution.**

480 **(a) Details on the matrix expansion mechanism. (a-1):** demethyl-esterified pectin chain at
481 rest in equilibrium with DM pectin molecules in solution (light blue). **(a-2):** When loading
482 with a mild force the molecules constituting the chain are elastically deformed. Egg-box
483 structures are undeformed and the corresponding bond strong. **(a-3):** If the loading force is
484 high enough (above a threshold value defined as $f_{th} = E_b/a$), egg-box structures are
485 mechanically deformed, their corresponding strength is lowered. Consequently, they can be
486 destabilized by close-by, demethyl-esterified pectin molecules in solution. **(a-4):** Once the
487 initial bond broken, the destabilizing molecule is inserted, increasing the total length of the
488 chain. **(b) Influence of cellulose microfibrils orientation. (b-1):** Structural sketch of a
489 fiber reinforced hydrogel. The big purple bars represent cellulose microfibrils, the smaller
490 orange one pectin strand composing the solid phase and the blue dots stand for the free pectin
491 molecules in the liquid phase. We assume that cellulose fibrils are deposited by a preferred
492 direction. Within this 2D representation, two 1D cases are evoked: **(b-2):** The studied pectin
493 strand is perpendicular to the cellulose microfibrils main direction. In that case, the two
494 structure can be assume in series and the forces they experience are the same: $f_{tot y} = f_c y =$
495 f_y where those forces respectively correspond to the total force felt by the wall, the fraction
496 felt by the cellulose fiber and the fraction felt by the pectin strand. **(b-3):** The studied pectin
497 strand is parallel to the main cellulose microfibrils direction. The total force exerted on the
498 wall is distributed between both structures, this time in parallel: $f_{tot x} = f_c x + f_x$; the

499 fraction felt by the pectin strand is consequently lower than the total force: $f_x \leq f_{tot x}$.

500 **Figure 2: Phase diagram of an hydrogel under tensile force.**

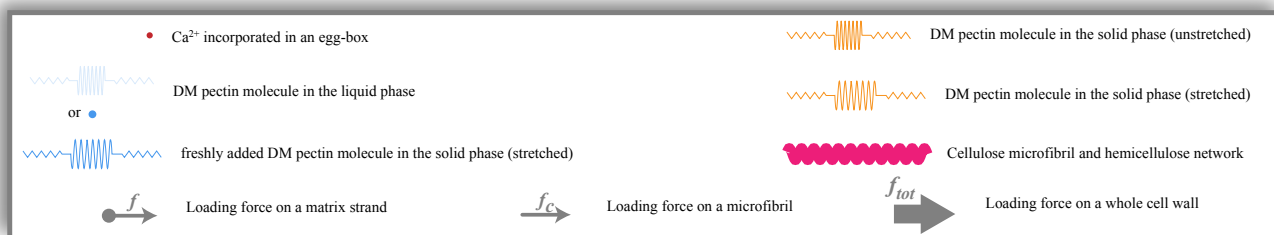
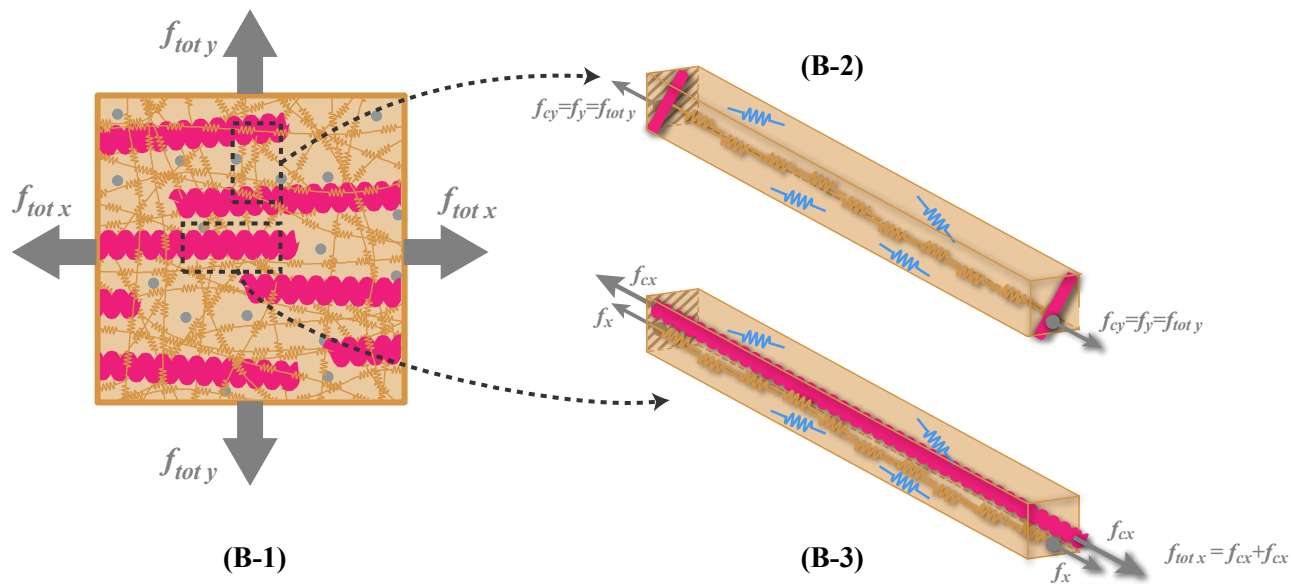
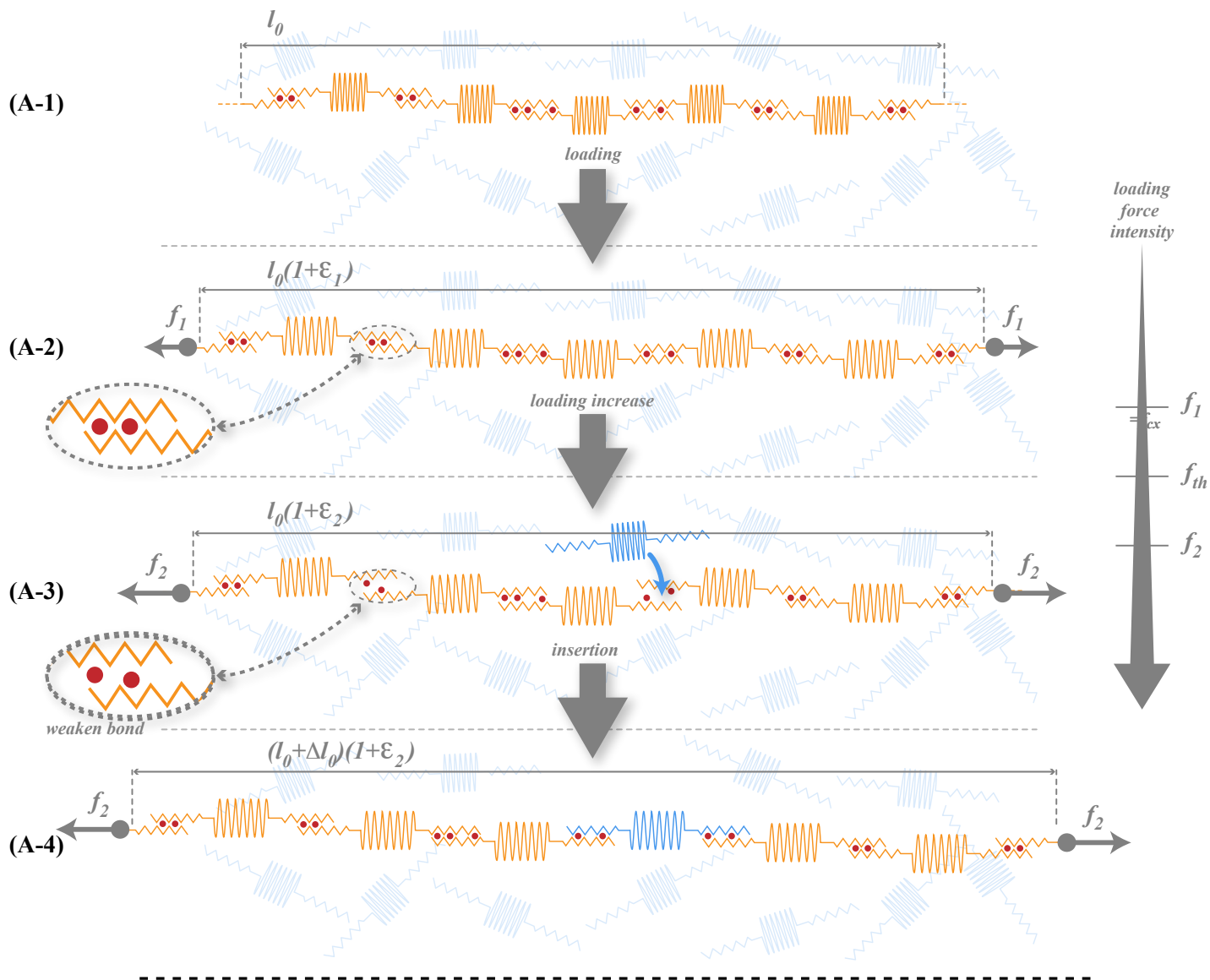
501 The abscise axis quantifies the work developed by the tensile force ($w = f \cdot a$) compared to the
502 thermal energy available ($\beta = 1/k_B T$). The ordinate axis shows the normalize concentration of
503 free active pectin molecules in the liquid phase. The orange curve is a visual representation of
504 Eq.3 and therefore represents the chemical equilibrium between the solid and the liquid phase of
505 the gel. Each point of the plane represents one configuration of the gel that corresponds to a
506 specific couple “*concentration / force*”, the points under the equilibrium curve correspond to gels
507 that do not expand their solid phase whereas points above do. Sub-figures **(a)** & **(b)** show two
508 simple putative growth scenarios: **(a)** From an initial non-growing state (black dot) we assume an
509 increase of the mechanical load, that translates onto the phase plan as a rightward shift of the
510 point describing the system state (gray dot). Being this time in the “growth zone”, spontaneous
511 insertion of monomers into the solid phase spontaneously happens. Note that from the initial
512 black point it takes a minimal force (dashed part of the arrow) to get into the “growth zone”, this
513 can be interpreted as a force threshold f_{th} , depicted by the vertical dotted orange line. Finally the
514 gray dashed arrow symbolizes the “out of equilibrium” driving force of the polymerization
515 process that tends to diminish the concentration of free molecules in solution. Note that if the
516 mechanical force goes back to its initial value (plain gray arrow), the system does not recover its
517 initial state (black dot) but a new one (orange dot). **(b)** This time growth is initiated by a release
518 of demethyl-esterified pectin in the liquid phase, again a threshold phenomenon is observed, this
519 time in terms of concentration c_{th} , depicted by the horizontal dotted orange line.

520 **Figure 3: Growth rate dependency on demethyl-esterified pectin**
521 **concentration, turgor pressure and temperature; comparison**
522 **between experimental data and model.**

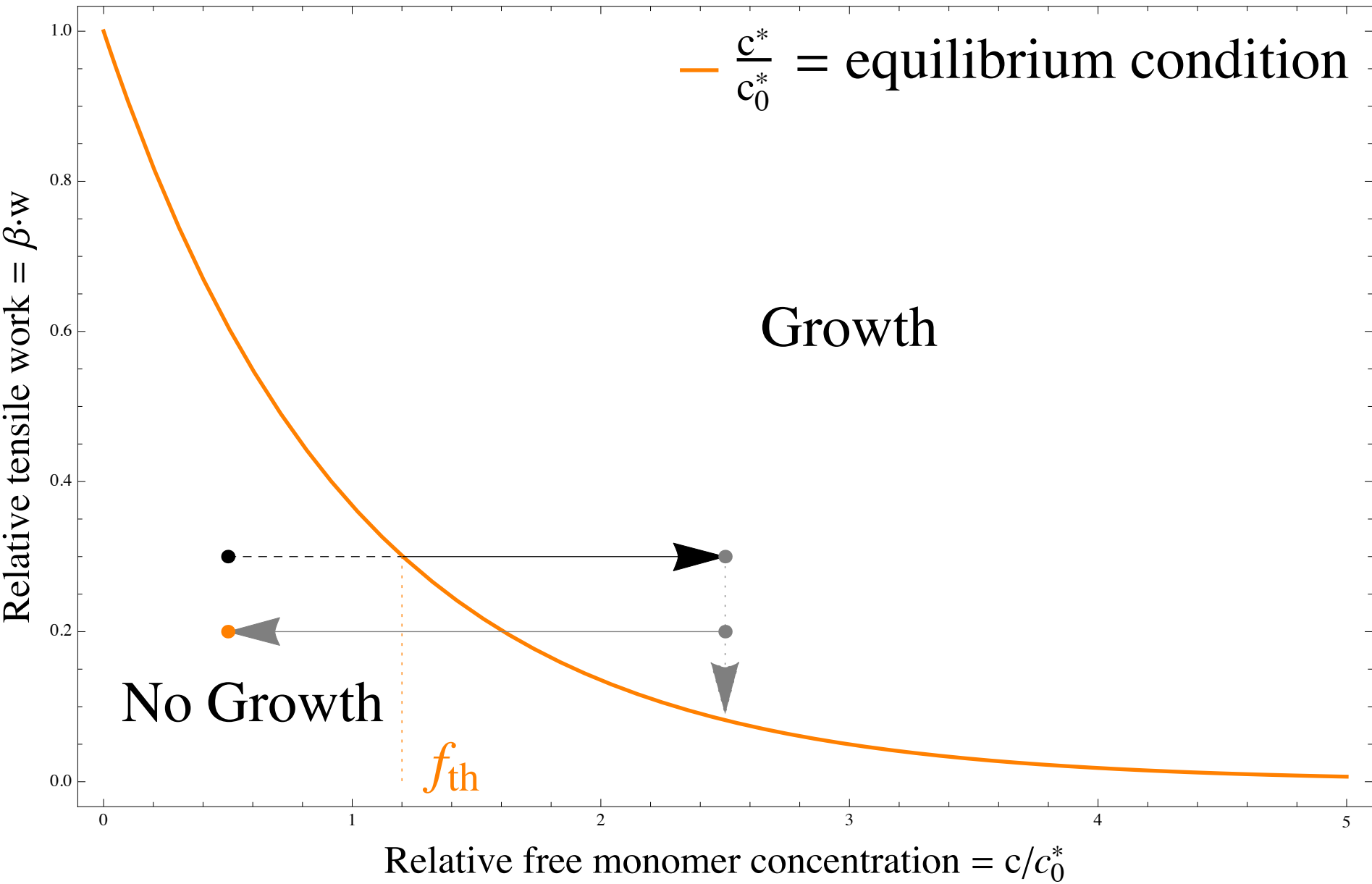
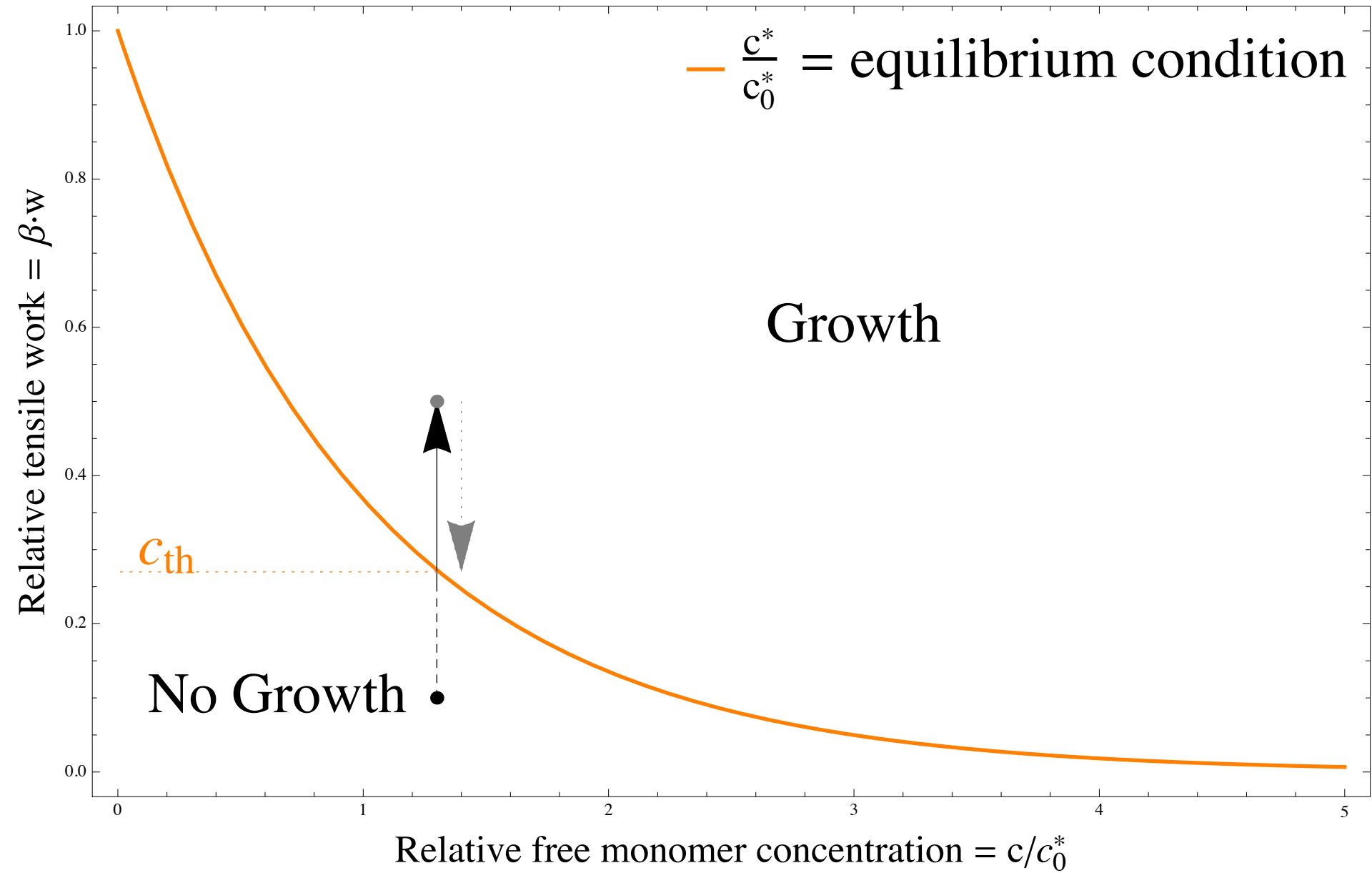
523 **(a): Influence of turgor pressure on relative expansion rate.** Comparison between
524 experimental data and Eq.4. Dots represent experimental published data from (Proseus *et al.*
525 2000) and error bars the precision of our reading of these data. The dashed curve represents the
526 best fit of these points by the exponential function exposed in Eq. 5: $R_g/R_g^0 = \exp(C_1 \Delta P_0 \cdot$
527 $(\Delta P/\Delta P_0 - 1))$ where C_1 is the fitting coefficient. ΔP_0 and $R_g^0 = R_g(\Delta P_0)$ are arbitrary values
528 taken as references. **(b)&(c):** Qualitative influence of various parameters on the growth behavior.
529 **(b): Influence of an increase of free demethyl-esterified pectin concentration in the liquid**
530 **phase (δc in Eq.4).** As on sub-figure (a), the curves depict the evolution of a normalized growth
531 rate R_g/R_g^0 with respect to a normalized pressure differential ($\Delta P/\Delta P_0$) and mimic Fig.3B
532 in [45]. The plain curve corresponds to the best-fit curve exposed on sub-figure (a). The dashed
533 curve is deduced from the plain one by a two-fold increase of the free demethyl-esterified pectin
534 concentration (δc). **(c): Influence of the temperature.** This time the temperature dependency
535 exposed in Eq.4 is investigated. P_0, T_0 and $R_g^0 = R_g(\Delta P_0, T_0)$ are still arbitrary reference values.
536 The plain curve corresponds to the best-fit curve exposed on sub-figure (a). The dashed curve is
537 deduced from the plain one by using a smaller value of the temperature similar to the drop of
538 temperature studied by Proseus *et al.* in [44], see Fig.13-B.

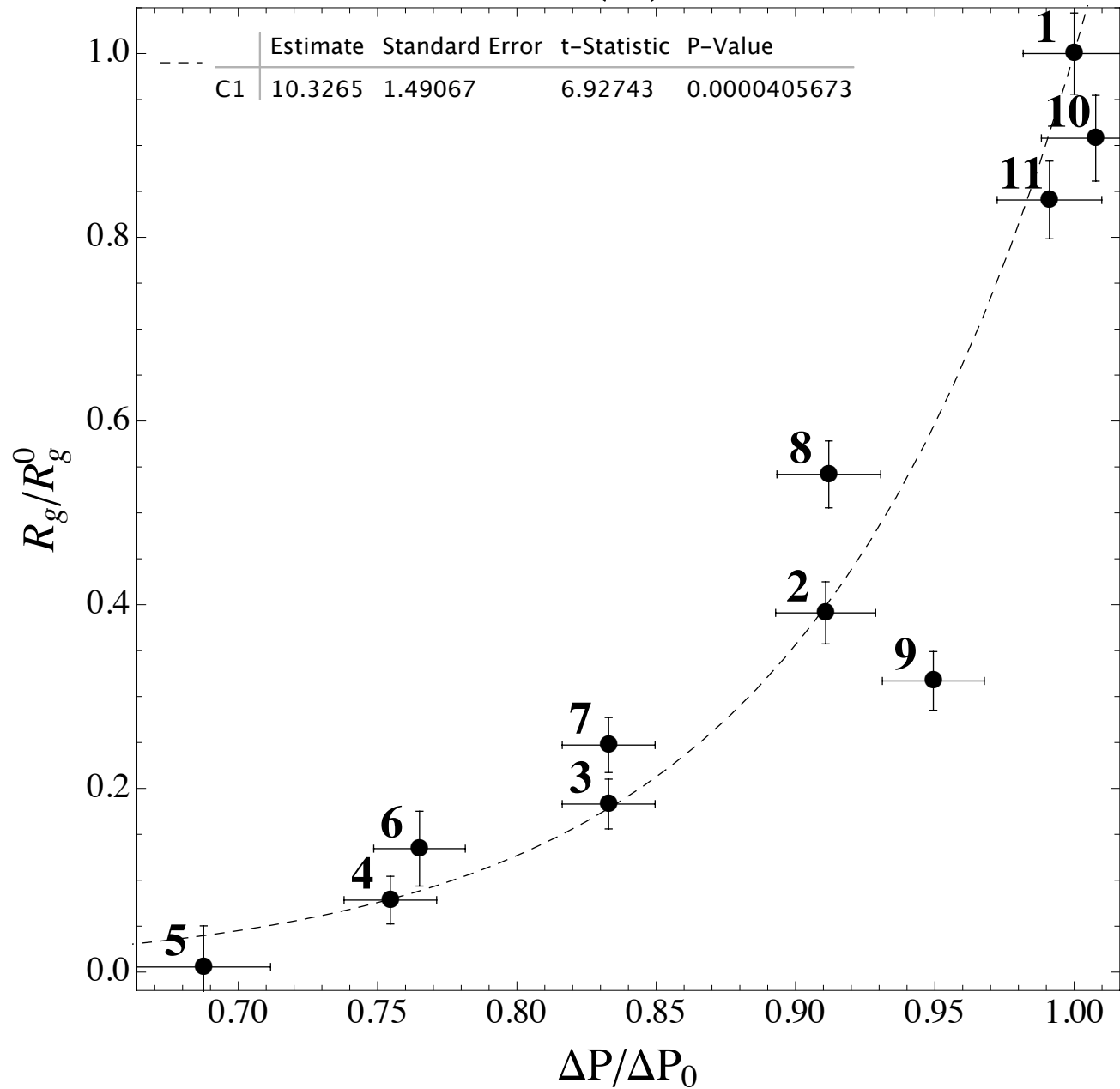
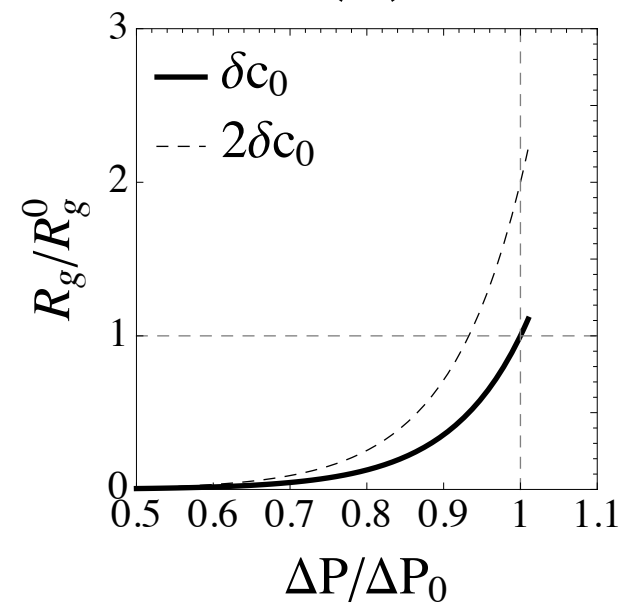
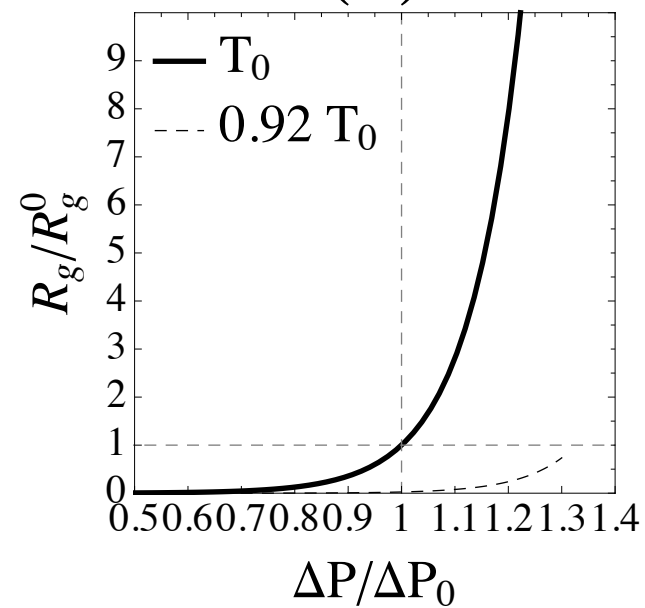
539 **Figure 4: Transducing chemical & mechanical inputs into**
540 **morphological outputs**

541 The morphological evolution of the tissue is quantified by its relative growth rate R_g . The growth
542 law that relates it to turgor-induced mechanical forces and to the cell wall mechano-chemical
543 properties is a direct consequence of the cell wall molecular organization. Its expression exposed
544 here corresponds to the combination of Eqs.4 & 5. From a functional perspective the growth law
545 can be seen as the final step of the integrative chain between gene expression and shape
546 evolution. It also appears as the step where biochemical properties (quantified by scalar variables,
547 *i.e.* « simple » numbers) are combined with mechanical and geometrical properties (quantified by
548 oriented variables, namely vectors and matrices).

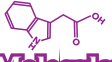


Key Figure

(A)**(B)**

(A)**(B)****(C)**

Molecular



Hormonal signalling



Genetic network



Post transcriptional regulation:
CMTs network dynamics
Enzymatic activity
Osmotic pressure regulation



Cell wall properties:
CMFs/HGs density & orientation
Pectin matrix properties



Shape

Cellular

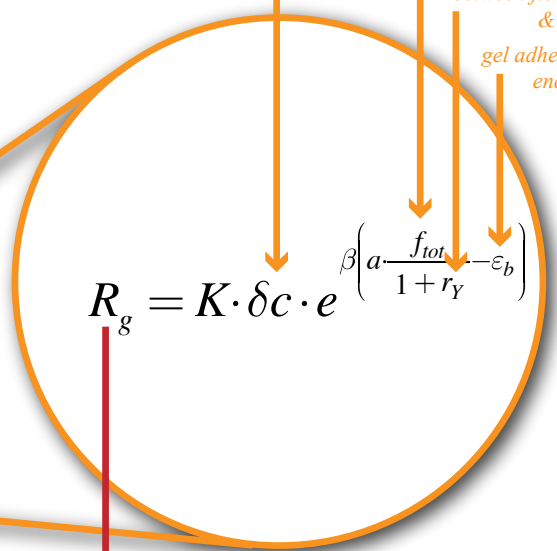


Tissular



Mechano-chemical inputs:

- Free DM-pectin concentration*
- Turgor-induced forces*
- Rigidity ratio between fibers & gel*
- gel adhesive energy*



$$R_g = K \cdot \delta c \cdot e^{\beta \left(a \frac{f_{tot}}{1 + r_Y} - \epsilon_b \right)}$$

Geometrical output:
Deformation field time evolution

